Implantation temperature dependence of electrical activation, solubility, and diffusion of implanted Te, Cd, and Sn in GaAs

Pearton, S. J.; Williams, J. S.; Short, K. T.; Johnson, S. T.; Jacobsen, D. C.; Poate, J. M.; Gibson, J. M.; Boerma, D. O.

Published in:
Journal of Applied Physics

DOI:
10.1063/1.343044

Implantation temperature dependence of electrical activation, solubility, and diffusion of implanted Te, Cd, and Sn in GaAs

S. J. Pearton, J. S. Williams, K. T. Short, S. T. Johnson, D. C. Jacobsen, J. M. Poate, J. M. Gibson, and D. O. Boerma

Citation: Journal of Applied Physics **65**, 1089 (1989); doi: 10.1063/1.343044
View online: https://doi.org/10.1063/1.343044
View Table of Contents: http://aip.scitation.org/toc/jap/65/3
Published by the American Institute of Physics

Implantation temperature dependence of electrical activation, solubility, and diffusion of implanted Te, Cd, and Sn in GaAs

S. J. Pearton
AT&T Bell Laboratories, Murray Hill, New Jersey 07974

J. S. Williams
Royal Melbourne Institute of Technology, Melbourne, Victoria 3001, Australia

K. T. Short
AT&T Bell Laboratories, Murray Hill, New Jersey 07974

S. T. Johnson
Royal Melbourne Institute of Technology, Melbourne, Victoria 3001, Australia

D. C. Jacobsen, J. M. Poate, and J. M. Gibson
AT&T Bell Laboratories, Murray Hill, New Jersey 07974

D. O. Boerma
University of Groningen, 9718 CM Groningen, The Netherlands

(Received 25 July 1988; accepted for publication 28 September 1988)

The relationship between electrical activity, dopant solubility, and diffusivity was investigated as a function of the substrate temperature during implantation of Te, Cd, and Sn ions into GaAs. Implant doses of these species in the range 5×10^{12}–5×10^{15} cm^{-2} were performed in the temperature range -196 to 400 °C, followed by either transient (950 °C, 5 s) or furnace (450–900 °C, 20 min) annealing. The redistribution after such annealing was found to depend on the implant temperature, and was always greatest for Cd followed by Sn and Te. The degree of electrical activation was in the same order, but there was essentially no correlation of electrical activity with dopant solubility. Te, for example, showed soluble fractions of ~90% for a dose of 10^{15} cm^{-2} after annealing at 850 °C or higher, regardless of the initial implant temperature. By sharp contrast, the electrically active fraction under these conditions was in the range 0.8%–3.4%. There was also no apparent correlation of the degree of electrical activity with the presence of defects visible in transmission electron microscopy. The energy required to activate the implanted ions fell broadly into two categories: "low" values in the range ~0.4–0.8 eV (which included Cd implanted or annealed under any condition, and elevated temperature implants of Sn and Te), and "high" values in the range 1.7–1.9 eV [which included implants of Sn and Te performed at -196 °C, or high dose (10^{15} cm^{-2}) room-temperature implants of these species].

I. INTRODUCTION

Ion implantation is used for two purposes in GaAs.[1–7] The first is to create doped regions, often selectively, by implantation into a partially masked substrate. The second is to destroy doping through the introduction of damage-related deep levels which trap charge carriers and are not thermally ionized at normal device operating temperatures. Once again, this is usually done in a selective manner to provide high resistivity regions between adjacent devices. The relatively slow maturation of a direct ion implantation technology for GaAs is due in at least some part to a lack of understanding of the relationship between electrical activity, dopant solubility, remnant damage, and dopant diffusivity upon annealing. Indeed, relatively little attention has been paid to the relationship between the solubility of implanted dopants in III-V semiconductors and their associated electrical activity. In Si, for example, there is generally a one-to-one correspondence between the occupation of a substitutional lattice position and electrical activity. By contrast it has previously been made clear that in GaAs, substitutionality of an implanted dopant is a necessary but not sufficient condition for electrical activity.[2,8] It is obviously necessary to gain more insight into the factors controlling the degree of electrical activation, particularly under the conditions in which this is much less than the corresponding soluble fraction.

In the case of donor species implanted into GaAs, it is well established that the maximum electron concentration after annealing is limited to $< 10^{19}$ cm^{-3}, and that the degree of electrical activity is dependent on the implantation temperature.[6] Sette *et al.*[9,10] have established a unique site, for example, for *S* which accounts for its lack of electrical activity. By contrast, hole concentrations in excess of 10^{20} cm^{-3} are achievable by acceptor implantation and subsequent annealing, and there is little effect of implant temperature upon the degree of activation. Also, in general, the donors show little redistribution during annealing, whereas there is marked diffusion of all the acceptor species during high-temperature treatments. An understanding of these effects can only be achieved by using a variety of techniques to correlate the structural and electrical properties of implanted layers in GaAs.

In this work we have systematically varied the critical

 0021-8979/89/031089-10$02.40

implant parameters, specifically ion dose, implant temperature, and annealing temperature, for three species—Cd, Sn, and Te. The choice of these dopants was dictated by their similar masses, which leads to similar amounts of lattice disorder introduced during implantation, and their electrical nature in GaAs. Tellurium is an As-site donor, while Cd is an acceptor occupying the Ga sublattice. Tin, on the other hand, is an amphoteric species capable of occupying either sublattice, although in general it is observed to display donor characteristics because of a tendency to favor Ga sites. For each of these species we have systematically investigated the relationship between solubility and electrical activity after both rapid and furnace annealing. The dopant solubility was measured by ion channeling, and the corresponding electrical activity obtained from Hall effect and capacitance-voltage profiling. The defect structures remaining after annealing were investigated by transmission electron microscopy. A preliminary report on this work has appeared previously.[11]

II. EXPERIMENT

All of the implants were performed into undoped semi-insulating [$(2–5)\times10^7\ \Omega$ cm], (100) orientation GaAs wafers grown by the liquid encapsulated Czochralski method. To ensure reproducible starting conditions, the wafers were boiled in a variety of solvents and rinsed thoroughly in deionized water before being etched for 5 min in 5 H_2SO_4:1H_2O_2:1H_2O at 70 °C. This removes approximately 10 μm of material, including the slightly disordered region caused by the manufacturers final wafer polishing step.

The Cd, Sn, and Te implants were performed in a nonchanneling direction [7° tilt of the wafer relative to the surface normal, and a 15° rotation relative to the major (110) flat] at a fixed energy of 100 keV. The ion doses were varied from 5×10^{12} to 5×10^{15} cm^{-2}, with the wafers held at one of four different temperatures: −196, 25, 200, and 400 °C. Since some trouble was taken to ensure that the samples were in good thermal contact with the temperature-controlled stage, and the beam currents used were relatively low (0.2–1.0 μA cm^{-2}), we estimate these temperatures are accurate to within 25 °C of the maximum values reached during the implant, except for the highest doses used (5×10^{15} cm^{-2}). Most of the annealing treatments were performed in one of two ways. In the first, the samples were held at temperatures between 450–850 °C in a flowing As-H_2 ambient within a multizone quartz furnace, in which As vapor from a solid source at 420 °C was transported across the samples by a flow of Pd-diffused H_2. In this arrangement, the uncapped implanted surfaces of the wafers were further protected against As loss by placing them face down on other clean GaAs substrates. All of these anneals were for 20 min. The second common method involved rapid annealing within a Heatpulse 410 system[12] at 950 °C for 5 s under a flowing forming gas (9% N_2:10% H_2) ambient. Once again the implanted wafer surfaces were protected by placing them face down on clean substrates, the so-called proximity method.[13] We have previously observed that 850 °C is the optimum furnace annealing temperature for activating implants in GaAs, and similarly 950 °C for 5 s is the optimum rapid thermal anneal (RTA) condition. Our measurements of activation kinetics have indicated that in many respects an RTA treatment for a few seconds is equivalent to a furnace anneal at a temperature of 50–100 °C lower. Selected samples were laser annealed with a 30 ns (FWHM) pulsed ruby laser beam at an energy density of 0.56 J cm^{-2} to compare activation under ultrafast annealing conditions with the more conventional methods. These laser irradiations were performed in air using a quartz lightpipe to homogenize the beam. In all of our annealing methods we avoided the use of encapsulating surface layers with their attendant disadvantages. For the purposes of our study it was felt important to minimize possible enhanced diffusion effects arising from the different thermal expansion coefficients of the encapsulant and GaAs, or of the possible preferential loss of one or other of the lattice constituents during annealing with a capping layer in place.

The solubility of the implanted dopants was obtained from 2-MeV He ion channeling measurements, and as is the usual convention we defined solid solubility to mean near-substitutional location of dopants.[8] Hall measurements were performed by alloying HgIn eutectic at 400 °C for 60 s to the corners of van der Pauw geometry samples (5×5 mm^2) of the annealed material. To obtain carrier density profiles we performed differential Hall measurements by a progressive measure-etch procedure using a calibrated etchant (1H_2SO_4:1H_2O_2:100H_2O) to remove controlled amounts of material ($\sim$35 A s^{-1}). On a number of samples we also measured the carrier profiles by electrochemical capacitance-voltage profiling on a Polaron PN 4200 system. For samples implanted with low ion doses and annealed at temperatures in excess of 750 °C, we had good success with this method, but in high dose implanted material we generally found that the remnant damage was sufficient to lower the minority-carrier lifetime to the point where the standard electrochemical etches were inoperative, necessitating the use of the differential Hall method for carrier profiling. In those cases in which both techniques were usable we found good agreement between them, typically less than a 15% variation in both the carrier concentrations and depths. The atomic profiles of the implanted dopants before and after annealing were obtained from secondary ion mass spectrometry (SIMS) measurements using Cs^+ ion bombardment in a Cameca IMS 3*f* system. The concentrations obtained by this method are estimated to be accurate to $\pm$ 30%, and the depth scales to $\pm$ 7%. Selected samples were also examined by plan-view transmission electron microscopy (TEM) to determine the type and density of the damage remaining after annealing.

III. RESULTS

A. Electrical activation

There was a marked contrast in the degree of electrical activity of the three species after annealing. For example, for a dose of 1×10^{15} cm^{-2} followed by annealing at 850 °C for 20 min, the sheet carrier density for Cd implants was a factor of 5 higher than for Sn, and a factor of 50 higher than for Te. A summary of the sheet carrier data for Cd as a function of

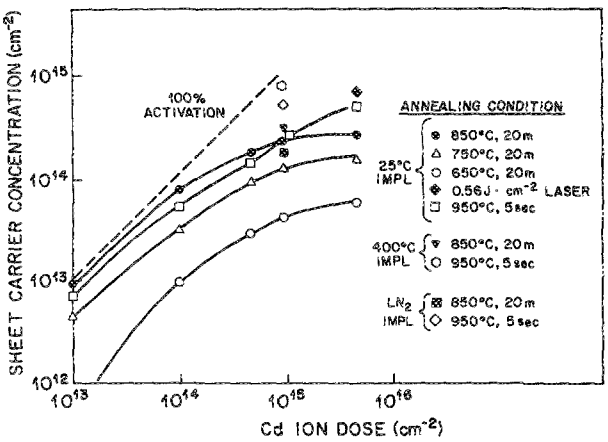

FIG. 1. Sheet hole concentration as a function of implant dose, implant temperatures, and annealing condition for Cd implanted in GaAs.

implant temperature, dose, and annealing condition is given in Fig. 1. The activation increases monotonically at moderate doses showing saturation effects only for doses near 10^{15} cm^{-2}. There was no particular advantage to the use of elevated temperature implants, and rapid annealing gave higher hole densities than furnace annealing for all implant temperatures. This appears to be a result of a lower degree of redistribution and less loss of Cd to the surface during shorter time anneals, as will be seen later.

Carrier profiles in Cd-implanted material after either furnace or rapid annealing are shown in Fig. 2. There is less redistribution in the latter case, resulting in higher peak hole densities. For both annealing methods, however, there is quite significant redistribution of the Cd, compared with the expected Gaussian-type profile, especially for the implants performed at room temperature and above. This is a result of two separate contributions. First, SIMS measurements on as-implanted samples (illustrated later) showed a long tail on the Cd distribution for implants performed at 200 or 400 °C. This is presumably a result of enhanced motion of Cd interstitials during the implantation step itself. The second contribution to the deeper profiles came from the annealing itself, and this again was more pronounced for the elevated temperature implanted samples. The mechanism in this case is not clear, but may be related to less trapping of interstitial Cd in samples with better initial crystalline quality, as is the case with the 200 and 400 °C implanted material in which amorphization was avoided.

The activation of Sn was consistently lower than that of Cd, as shown in Fig. 3. We saw no electrical activity after 650 °C furnace annealing for any of the doses investigated, and activation percentages of only 10% for 10^{15}-cm^{-2} dose implants annealed at 750 °C and above. Once again there was no particular advantage to the use of elevated temperature implantation as judged by a comparison of sheet electron density after equivalent anneals. The implanted layers displayed *n*-type conductivity over the entire dose range investigated. There was also no systematic trend as far as superior activation for either annealing method was concerned. The saturation in electrical activity for Sn as a function of dose is quite marked even for the highest temperature anneals.

Carrier profiles after annealing of Sn implants, obtained by differential Hall measurements, are shown in Fig. 4. There are several obvious trends. First, profiles for elevated temperature implants are broader than for either room-temperature or liquid-nitrogen (LN_2) implants. Second, the peak carrier densities are essentially equivalent for furnace annealing of all implants except those performed at LN_2 temperatures. This trend is basically followed for rapidly annealed samples but here the room-temperature implants also show inferior activation compared with those implants performed at elevated temperatures. This may be a result of incomplete damage removal during the short duration anneal. As will be shown later the broad carrier profiles for samples initially implanted at 200 or 400 °C result from two contributions—diffusion during the implant step itself, and diffusion during the subsequent annealing treatment. It is

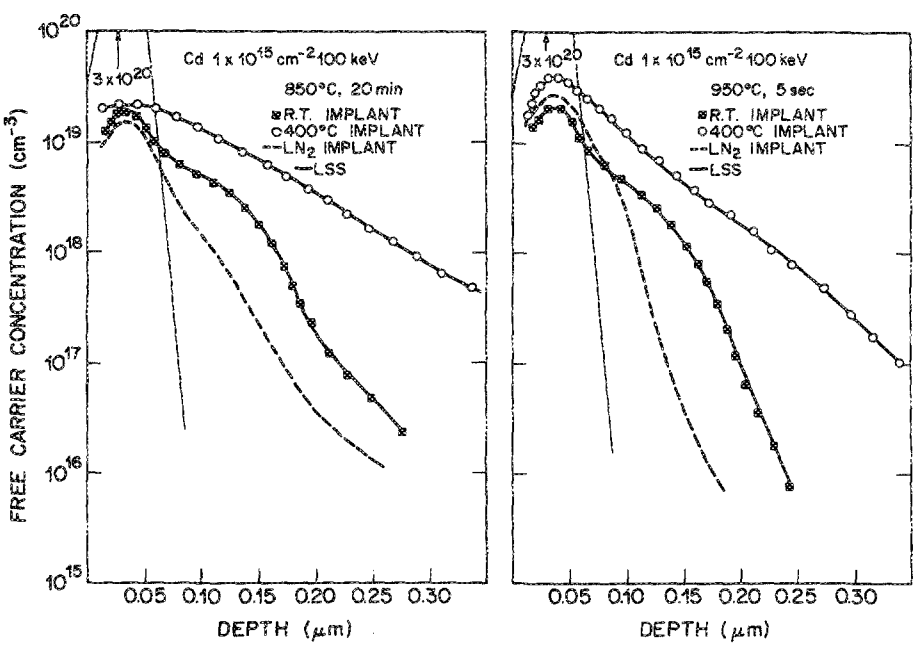

FIG. 2. Carrier profiles in Cd-implanted GaAs (1×10^{15} cm^{-2} at 100 keV) after furnace (right) or rapid (left) annealing. These were obtained by differential Hall measurements.

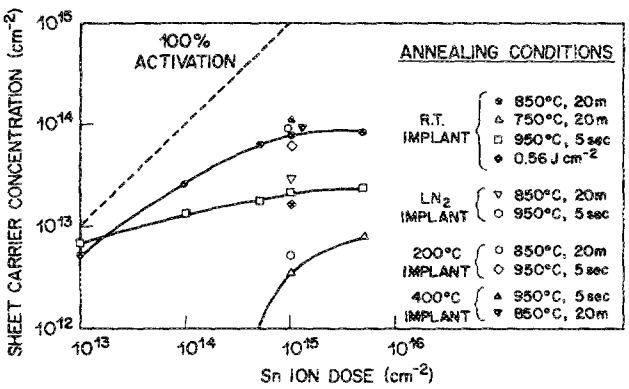

FIG. 3. Sheet electron densities as a function of implant dose, implant temperature, and annealing condition for Sn implanted in GaAs.

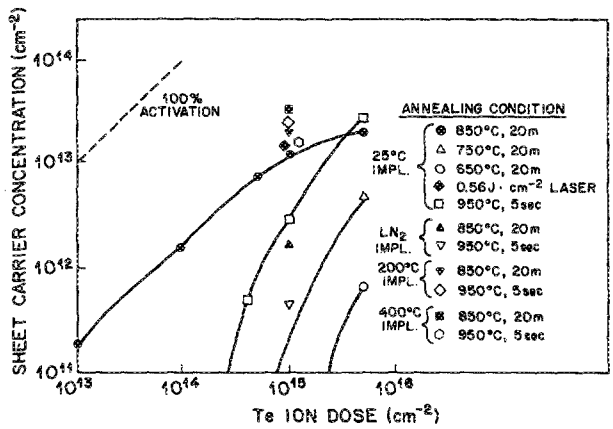

FIG. 5. Sheet electron densities in Te-implanted GaAs as a function of implant dose, implant temperature, and annealing condition.

worth noting at this point that the peak electron concentration obtained by room-temperature Sn implantation ($\sim 7\times 10^{18}$ cm^{-3}) is larger than that typically obtained by similar implants of a lighter and more commonly used donor species, namely Si. Peak carrier concentrations obtained by room-temperature Si implants are generally limited to $(2–4)\times 10^{18}$ cm^{-3}, although values as high as 6×10^{18} cm^{-3} have been reported.[14]

The case of Te implantation also shows some interesting trends in terms of electrical behavior. As shown in Fig. 5, the activation is particularly low, of the order of 1% in all cases. The activation improves for elevated temperature implants, and is always higher for furnace annealing over rapid annealing. It is possible this is related to more complete damage removal in the former case, consistent with the higher activation for the elevated temperature implants. This effect is not as obvious for lighter donor species such as Si.

The carrier profiles in samples implanted with Te at a dose of 1×10^{15} cm^{-2} are shown in Fig. 6. The peak carrier densities are in agreement with the sheet measurements, with the highest values for elevated temperature implants and furnace annealed samples. There is relatively little redistribution upon annealing for either annealing method when an estimate is made of the as-implanted profile from the Transport of Ions in Matter (TRIM) code,[15] consistent with the low diffusivity for the other donor species in GaAs.[1,3]

We also measured the activation energy required to achieve carrier activation of the three different implanted species. This was measured for low doses (5×10^{13} cm^{-2}) and high doses (1×10^{15} cm^{-2}) from the slope of an Arrhenius plot of sheet carrier concentration against inverse annealing temperature. Examples of these measurements are shown in Fig. 7. The kink in the Cd data represents a saturation in electrical activity with annealing temperature. The complete set of data is summarized in Fig. 8, and it can be seen that the values fall broadly into two categories—those which we will designate as low energies (0.4–0.8 eV) and those with high values in the range 1.7–1.9 eV. Within the former category fall all of the Cd implants, regardless of dose or implant temperature, and also elevated temperature Sn

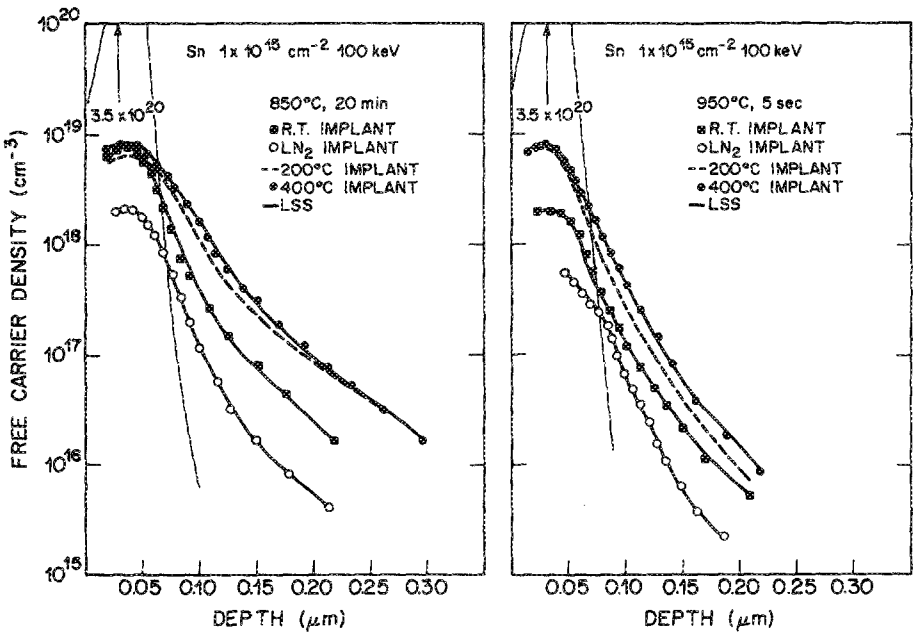

FIG. 4. Carrier profiles in Sn-implanted GaAs (10^{15} cm^{-2} at 100 keV) after furnace annealing (right) or rapid (left) annealing.

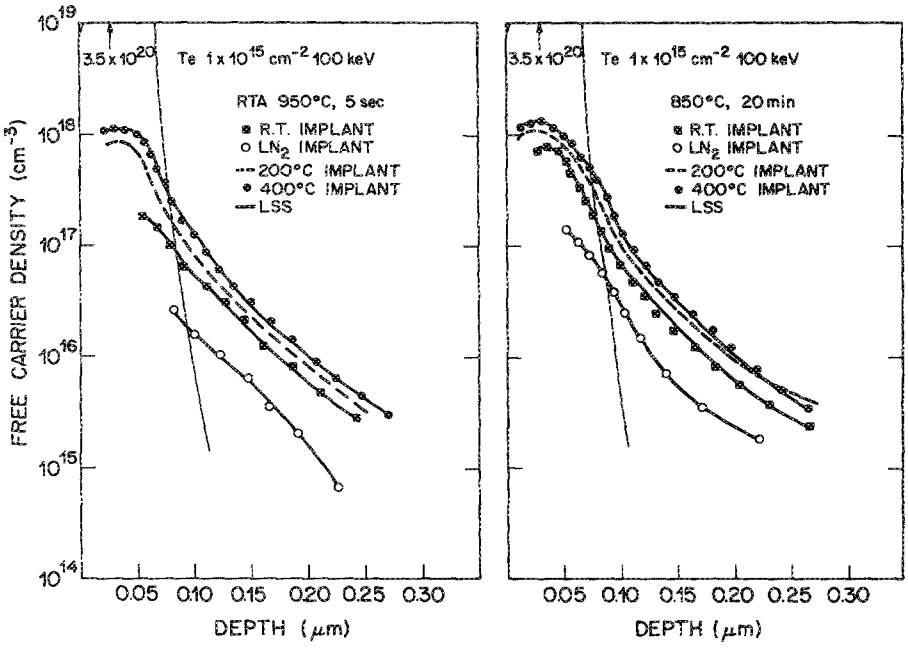

FIG. 6. Carrier profiles in Te-implanted GaAs (10^{15} cm^{-2} at 100 keV) after furnace (right) or rapid (left) annealing.

and Te implants. The second category includes all high dose implants of Sn and Te performed at room temperature or − 196 °C, and most of the lower dose implants of these species at the same temperatures. As a comparison we have previously measured the activation energy for Si activation for doses of 10^{15} cm^{-2} by both rapid and furnace annealing. In both cases the value was 0.51 eV (Ref. 16) consistent with the value obtained by Hiramoto, Saito, and Ikoma[17] for lower dose (3×10^{13} cm^{-2}) Si implants. Barret *et al.*[18] obtained a value of 1.2 eV for electrical activation of the heavier donor Se. We also measured a low value (0.70 eV) for Be activation, while Kular *et al.*[19] obtained a value of 0.53 eV for Zn activation.

We may well ponder the physical meaning behind these two broad categories of carrier activation energies. The low values include all of the acceptor dopants, which show high levels of activation in GaAs even for relatively low annealing temperatures or for high doses. This is presumably a result of high substitutional fractions of uncomplexed acceptors for these conditions. By contrast the high values of activation energy are associated with donor implants in which the electrically active fraction after annealing is far below the total implanted dose. In addition, low-temperature Hall measurements show near-complete compensation in such samples,

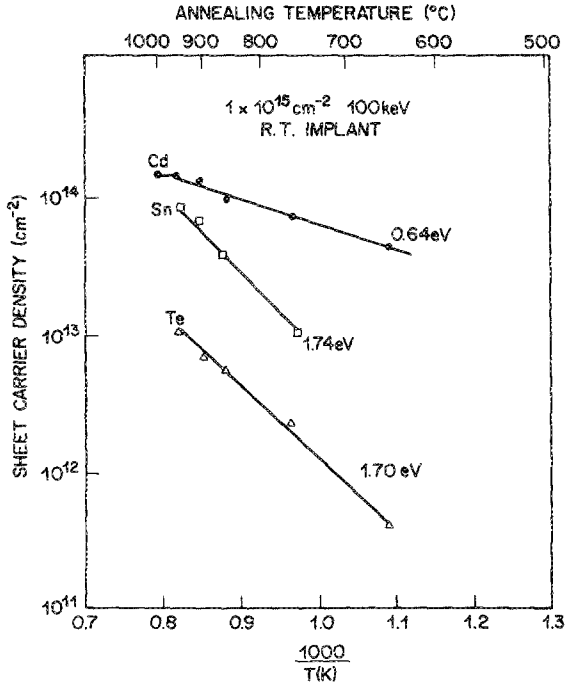

FIG. 7. Temperature dependence of carrier activation in Cd-, Te-, or Sn-implanted GaAs wafers (dose = 10^{15} cm^{-3}) annealed for 20 min at the temperatures shown.

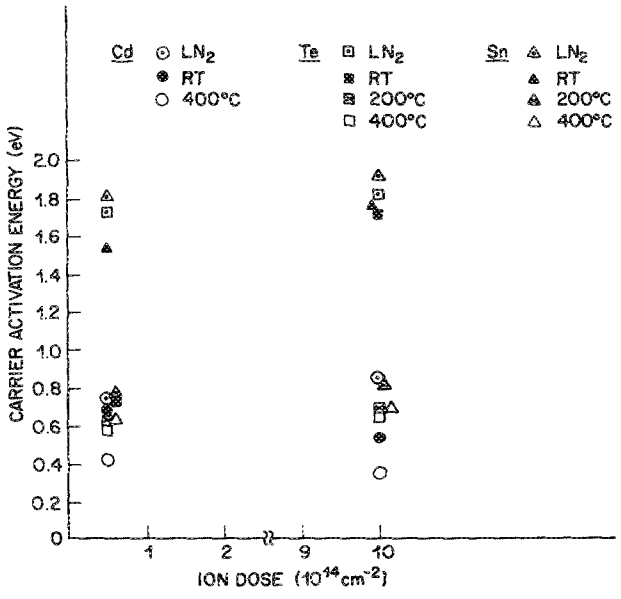

FIG. 8. Thermal activation energy required to achieve carrier activation in Cd, Te, or Sn implanted in GaAs, as a function of ion dose and implant temperature.

indicating the presence of essentially equal numbers of implantation produced donors and acceptors.[9-11,19-24] We will see later that the substitutional percentage of donors in most cases is very high, and therefore the question is why is the electrical activity so low. The answer probably lies in the formation of stable donor-vacancy complexes which show acceptor behavior, leading to self-compensation of the donors.[9,10,20] We will return to this point in the discussion section, as it appears to occur with all implanted donors in GaAs, and controls the level of activation achievable by implantation.

We note also that Sealy and co-workers[21-23] have proposed that low values of activation energy are associated with motion of the implanted species to an isolated substitutional lattice site, whereas the high values would correspond to the breakup of the complexed donor-vacancy defects. This proposal is certainly consistent with the high electrical activity in the case of implanted acceptors at virtually any dose or of donors at low doses. The formation of vacancy-donor complexes is significant only for high doses, corresponding to high values of activation energy.

B. Redistribution during implantation and annealing

A comparison of the atomic profiles of the three species before and after furnace annealing at 850 °C for 20 min is shown in Fig. 9. The implants in this case were done at room temperature. There is little motion and no loss of either Sn or Te during the annealing treatment, but most of the Cd is preferentially lost to the surface. However, as can be seen from the electrical profiles in Fig. 9, essentially all the Cd that remains is electrically active. We have previously reported similar behavior for high dose Be and Mg implants in GaAs after both furnace and rapid annealing.[24] The interesting feature of this redistribution is that there is only limited diffusion of Cd or the other acceptors into the bulk. The electrical activity of both Sn and Te is relatively poor, ~10% for Sn and ~1% for Te. As expected, we saw even less redistribution of all of these species for rapid annealing compared to furnace annealing. This was true for the entire range of implant temperatures investigated.

The effect of the wafer temperature during implantation on the as-implanted atomic profiles of Sn in GaAs is shown in Fig. 10. For the sample implanted at − 196 °C a thick amorphous layer was formed, and the Sn ion range distribution is near Gaussian, as predicted by classical LSS (Lindhard, Scharff, and Schiotts) theory.[24] For room-temperature implantation a considerably thinner amorphous layer was formed because of self-annealing, and a limited amount of Sn diffusion (or a channeling tail) was observed in this sample. Implantation at 200 or 400 °C prevented amorphization of the GaAs lattice, although the high dechanneling rate seen by Rutherford backscattering (RBS) in these samples indicated the presence of dislocations in the end-of-range region. For implantation at both temperatures, the unannealed Sn profile showed considerable diffusional broadening and/or partial channeling during implantation. The mobility of vacancies and interstitials created during the implant is expected to be high at these temperatures, and most likely assist motion of Sn.[4]

The trend of broader atomic profiles for samples implanted with Sn at elevated temperatures persists after subsequent rapid annealing, as also shown in Fig. 10. A low concentration tail on the Sn profile is particularly evident in the sample implanted at 400 °C. Electrical measurements on this sample showed that all of the Sn in this tail region was electrically active, while less than 10% of the Sn in the immobile, high concentration region near the surface was active. The fact that the mobile form of Sn, which presumably is not complexed with lattice defects or in a precipitated form, is highly electrically active is another piece of evidence linking the interaction of implanted donors with point defects as a controlling factor in determining their electrical behavior.

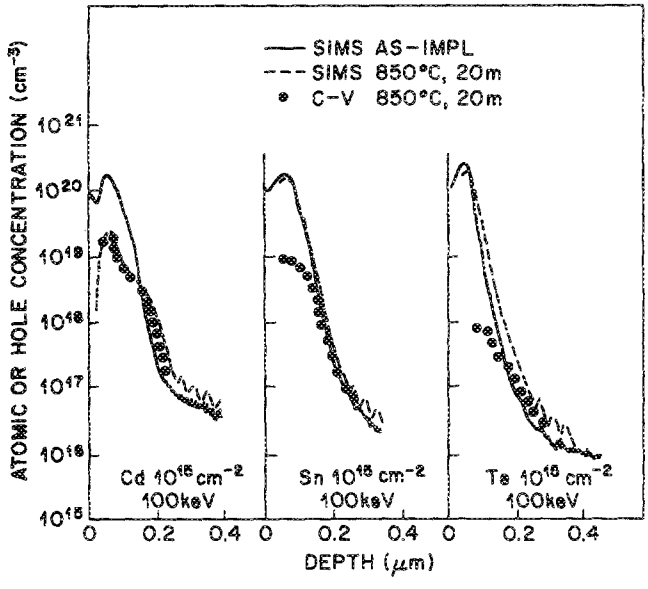

FIG. 9. Atomic profiles obtained by SIMS before and after furnace annealing (850 °C, 20 min) of Cd, Sn, or Te implanted in GaAs at room temperature. Also shown are the electrically active profiles after annealing.

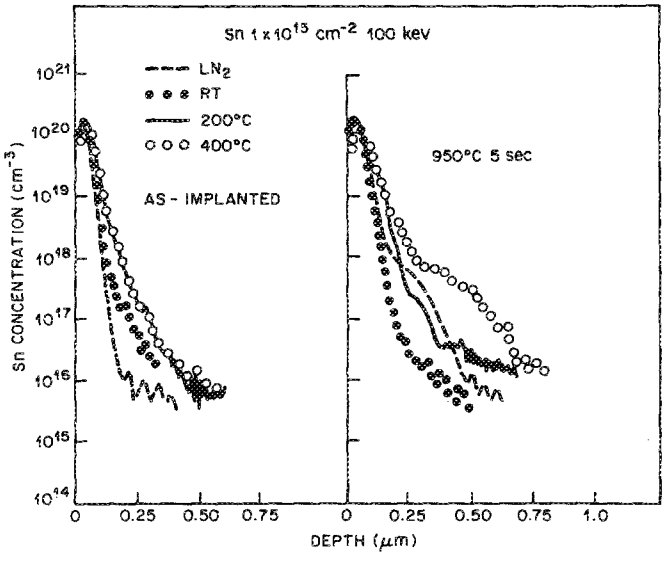

FIG. 10. Atomic profiles obtained by SIMS of as-implanted and rapidly annealed (950 °C, 5 s) samples implanted with Sn (10^{15} cm^{-2}, 100 keV) at four different temperatures.

C. Implantation annealing temperature dependence of solubility

The correlation between solubility of the implanted species and their electrical activity was investigated by taking ion channeling and Hall measurements on the same samples. Random and aligned orientation channeling spectra from the sample implanted with Sn (1×10^{15} cm^{-2}, 100 keV) at 25 °C are shown in Fig. 11. The aligned spectrum shows the near surface is amorphous after implantation, but regrows completely after either rapid or furnace annealing. The minimum backscattering yield in this material after both types of annealing was ~3.5%, identical to that in unimplanted GaAs. There is approximately 40% of the Sn substitutional after furnace annealing, and approximately 70% after rapid annealing at 950 °C.

The substitutional Sn fraction as a function of implant temperature and annealing condition is shown in Fig. 12, for a dose of 10^{15} cm^{-2} at 100 keV. There was no measurable substitutionality of the as-implanted Sn for − 196 or 25 °C implants. After annealing these samples the substitutional fractions ranged from 25% to 70%. This is expected behavior, namely that at least some of the implanted ions would become substitutional after removal of an amorphous layer during annealing. However, the opposite trend was observed for elevated temperature implantation. In these cases ~85% of the Sn was substitutional after implantation but this level of solubility was metastable, and Sn came out of solution upon annealing. The decrease in the soluble percentage is marked, falling to between 18% and 50%, depending upon the annealing condition. That there is no correlation between solubility and electrical activity is also evident from Fig. 12. The electrically active fraction is never higher than 10% of the implanted dose. Except for the implant performed at − 196 °C, rapid annealing gave higher solubilities than furnace annealing, and also less diffusion of the Sn for all implant temperatures.

It has previously been reported that for Sn implants performed at − 196 °C, the maximum solubility of ~2×10^{20} cm^{-3} occurred for 600 °C anneals.[8] Further annealing at 900 °C reduced this to ~10^{19} cm^{-3}. This is consistent with our present data, shown in Fig. 13. All of the samples show a decrease in Sn solubility for temperatures above 600 °C. We observed a maximum soluble concentration of 4×10^{20} cm^{-3} following 650 °C furnace annealing of a sample implanted with a dose of 5×10^{15} cm^{-2} Sn at 25 °C.[9,25] After annealing at 850 °C for 20 min the solubility fell to ~2×10^{20} cm^{-3}. The solubility of Sn depends on both the original temperature of the implantation and the subsequent annealing temperature.

The case of implanted Te is more straightforward than that of Sn. Once again we used ion channeling to measure the solubility of Te both before and after annealing. A typical RBS spectrum for a Te implant (5×10^{15} cm^{-2} dose) at 25 °C is shown in Fig. 14. For this very high dose the sample did not become amorphous during the implant, presumably because of beam-induced heating. After furnace annealing the crystalline quality of the sample is recovered, at least to the sensitivity of RBS (χ_{min} = 3.1%), and there is a soluble Te concentration of ~2.5×10^{21} cm^{-3}. This is a factor of

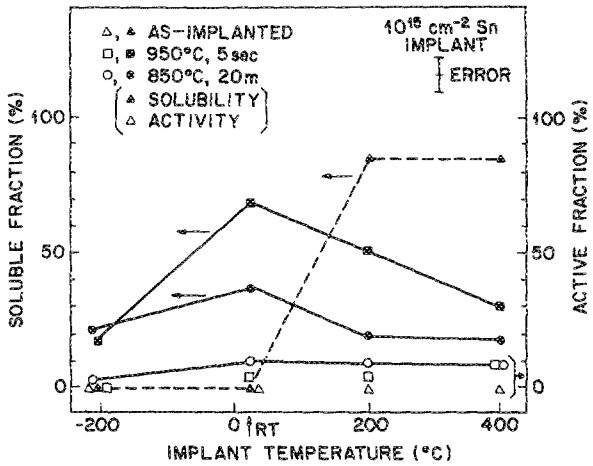

FIG. 12. Summary of Sn solubility data for 10^{15} cm^{-2}, 100-keV implants performed at four different temperatures. The electrically active fractions obtained from Hall data are also shown.

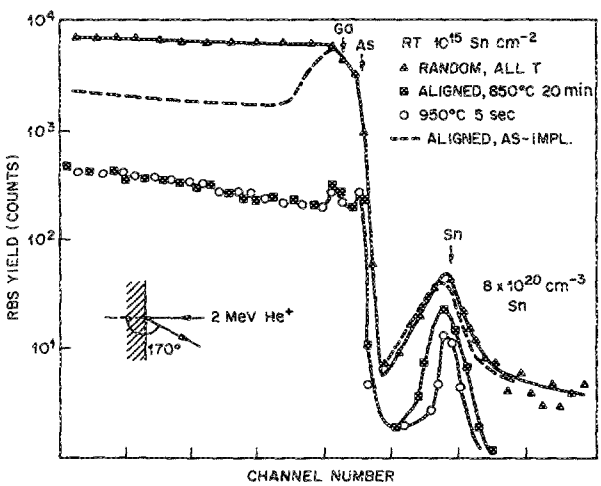

FIG. 11. Ion channeling spectra for GaAs samples implanted with Sn (10^{15} cm^{-2}, 100 keV) at 25 °C. The samples were subsequently annealed at 850 °C, 20 min or at 950 °C, 5 s.

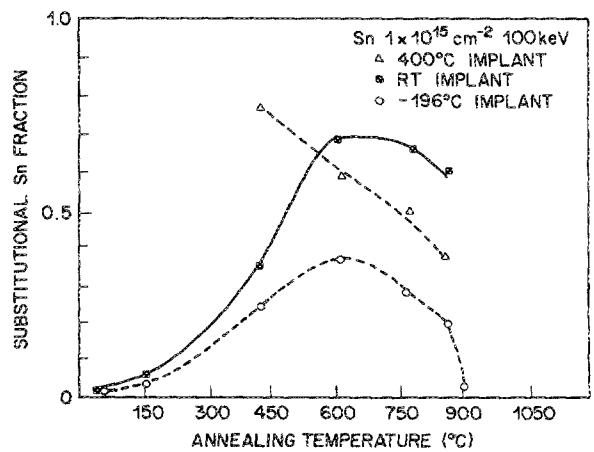

FIG. 13. Evolution of Sn solubility in samples implanted with a dose of 10^{15} cm^{-2} at 100 eV, as a function of post-implant annealing temperature (20-min anneals).

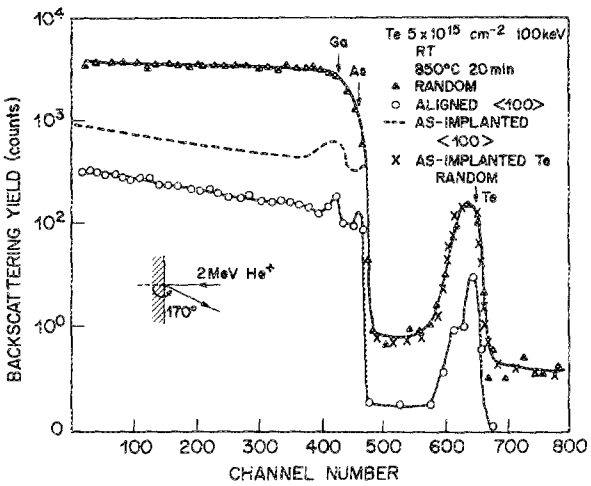

FIG. 14. Ion channeling spectra for GaAs samples implanted with Te (5×10^{15} cm^{-2}, 100 keV) at 25 °C. Annealing was performed at 850 °C, 20 min, or at 950 °C, 5 s.

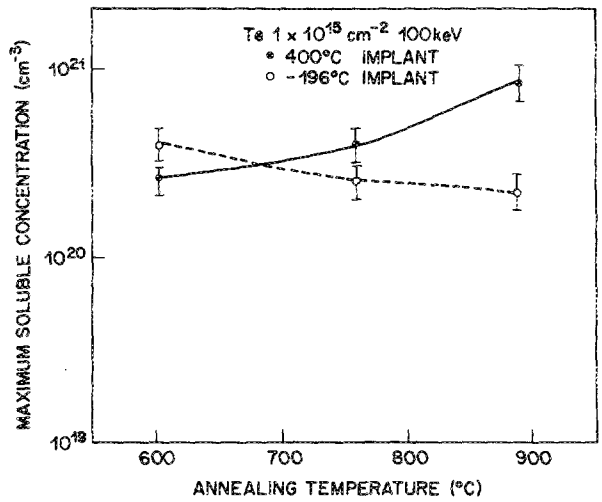

FIG. 16. Evolution of Te solubility in samples implanted with a dose of 10^{15} cm^{-2} at 100 keV, as a function of post-implant annealing temperature (20-min anneals).

~300 times higher than the electrically active concentration in the sample.[26]

The implantation and annealing temperature dependence of the Te solubility and electrical activity for a dose of 10^{15} cm^{-2} are shown in Fig. 15. There was no soluble fraction for room-temperature implants, but there was a high level (~90%) of substitutionality for elevated temperature implantation. There was no metastability upon annealing, with the soluble fractions remaining the same within experimental error. The soluble concentrations were at least two orders of magnitude higher than the electrically active fractions, which ranged from 0.8% to 3.4% depending on the experimental conditions. There was also little change in the soluble concentrations with annealing temperature, as shown in Fig. 16. The case of Cd was more difficult to quantify because of its extensive redistribution for annealing, even for elevated temperature implants. From somewhat limited data we observed high Cd solubility (≥50%) after all annealing treatments, with a concomitantly high electrically active fraction.

It is worth noting that the implantation induced damage in the GaAs after annealing should be approximately the same since the three implanted species have roughly the same mass. In all cases, implantation at −196 °C for a dose of 10^{15} cm^{-2} produced a thick amorphous layer which was essentially completely regrown after annealing. Typically, samples annealed by RTA showed more remnant disorder as measured by RBS than furnace annealed material. Implantation at 25 °C produced thinner amorphous layers which also regrew upon annealing, leaving dislocation loops clustered near the end of the ion range. Samples implanted at 200 or 400 °C with a dose of 10^{15} cm^{-2} did not become amorphous, but had high dechanneling rates, indicative of a high density of extended defects. Table I shows some representative minimum backscattering yields from GaAs implanted at various temperatures with Te, Cd, or Sn at a dose of 10^{15} cm^{-2}, after annealing at 650–950 °C. For either furnace or

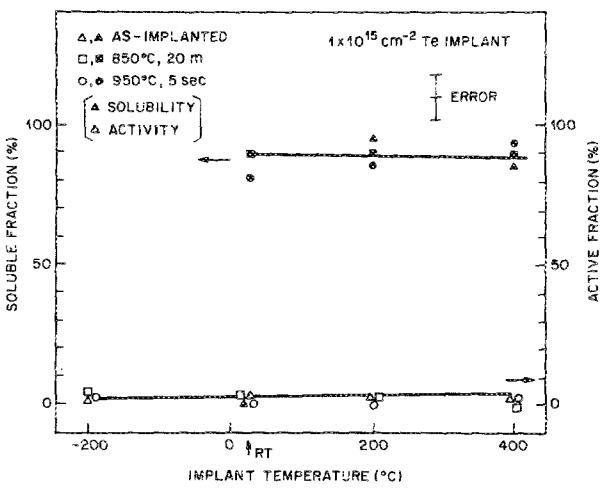

FIG. 15. Summary of Te solubility and electrical activity data for 10^{15}-cm^{-2}, 100-keV implants performed at four different temperatures and annealed either at 850 °C, 20 min or 950 °C, 5 s.

TABLE I. Representative He^+ ion backscattering yields (χ_{min}) in implanted GaAs (10^{15}-cm^{-2} dose).

Species	Implant temp. (°C)	Anneal temp (°C)	χ_{min} (%)
Cd	25	···	39.0
Cd	25	850 °C, 20 min	3.5
Cd	25	950 °C, 5 s	5.1
Te	25	···	25.0
Te	25	850 °C, 20 min	3.3
Te	25	950 °C, 5 s	3.3
Te	200	···	6.1
Te	200	850 °C, 20 min	3.9
Te	200	950 °C, 5 s	5.3
Te	400	···	6.0
Te	−196	950 °C, 5 s	15.0
Sn	25	···	28.0
Sn	25	850 °C, 20 min	3.4
Sn	25	950 °CC 5 s	3.1

rapid annealing the aligned RBS spectra for these samples resembled those of preimplant samples, but TEM micrographs showed the presence of a relatively high density ($\geq 10^8$ cm^{-2}) of defects remaining in the material. We prepared plan-view specimens of GaAs implanted at various temperatures with Te at a dose of 10^{15} cm^{-2}, and subsequently annealed at 650, 750, and 850 °C for 20 min, or at 950 °C for 5 s. For the highest annealing temperatures, in each case there was higher total defect densities after rapid annealing than after furnace annealing. An example comparing the effectiveness of the two methods in removing disorder is shown for Te-implanted samples in Fig. 17. There was no correlation between the amount of visible residual disorder in the annealed GaAs and the electrical acitivity of the implanted dopant.

IV. DISCUSSION AND SUMMARY

The solubility of Sn, Cd, and Te implanted in GaAs is a function of both the initial amount of damage created (determined by the wafer temperature during implantation) and the subsequent annealing temperature. The main points arising from the data are:

(1) There is no correlation between solubility and electrical activity for Sn or Te. By contrast, Cd appears to be both fully active and substitutional when it remains in the GaAs after annealing.

(2) The amount of activation follows the trend Cd > Sn > Te, i.e., acceptor > amphoteric species > donor.

(3) The amount of diffusion during annealing follows the trend for activation.

(4) There is no apparent correlation between activation and the amount of visible damage remaining in the implanted layer.

(5) Cd always shows a low activation energy required to electrically activate an implanted ion. For high doses ($\geq 5\times 10^{14}$ cm^{-2}) Te and Sn always show a high value for this activation energy. We take this to mean that Cd does not form stable complexes with point defects in the material.

The specific details for high doses of the three species may be summarized as follows[9]:

(1) Cd diffuses during implantation at elevated temperatures and during subsequent annealing. It appears to be highly soluble after all annealing conditions and in closer agreement with the level of electrical activity than for Sn or Te. There was significant loss of Cd to the surface for extended high-temperature annealing.

(2) The as-implanted Sn solubility is metastable, with the Sn coming out of solution as the annealing temperature is increased. The solubility is a function of the original implant temperature and the subsequent annealing temperature. There was no correlation of electrical activity with the Sn solubility. Sn diffuses during elevated temperature implantation, and slightly during annealing.

(3) For elevated temperature implants, or after annealing, Te is always highly substitutional. There was no correlation between solubility and electrical activity.

These results emphasize that it is difficult to quote solubilities for implanted dopants in GaAs, because they show a strong dependence on experimental conditions. To understand what determines the electrical activity of such dopants, it is necessary to know both their lattice site location and the bonding neighborhood around them. It appears to be the interaction of the implanted species with discrete point defects which determines their electrical activity. These defects may be created during the implant or annealing steps, or may already be present in the GaAs. Possible candidates which would effect implanted dopant activity are native defects such as As and Ga vacancies and antisite defects. In the case of amphoteric ions, like Sn, next-neighbor pairs with overall electrical neutrality probably play a role. From the activation kinetics it appears that Cd and other acceptors are relatively immune to defect interactions which reduce their level of activation. Hence, acceptors do not show a significant saturation in electrical activity with increasing dose in contrast to the behavior for donor implants. A clear reason for this will only be forthcoming by directly probing the acceptor neighborhood to reveal the differences between donors and acceptors.

On this question there have been recent extended x-ray absorption fine structure (EXAFS) measurements of the local atomic environment around implanted *S* and GaAs.[9,10] The results were consistent with the presence of two substitutional *S* sites of approximately equal concentration: one an unperturbed S_{As} site, and one a relaxed configuration with an S_{As} site associated with an As vacancy in the second neighbor position. Electrically, the former site would be a donor, and to explain the high level of compensation in the implanted layer, the second configuration must be an acceptor. This result was consistent with careful crystal doping experiments in which acceptors were also created upon donor doping, with their concentration tracking the added donor concentration. We assume that Te would behave in a similar way to *S*, and further assume that the As vacancies are created during the implantation step itself and migrate with annealing to react with the donor ions. It has previously been reported that arsenic vacancies are the predominant stable defects in irradiated GaAs, as determined from the anisotropy of damage production.[27] Furthermore, the Ga interstitials created are reported to be mobile even at 4 K, probably recombining with Ga vacancies or divacancies to give arsenic vacancies and V_{Ga}-Ga_{As} complexes.[27] Anneal-

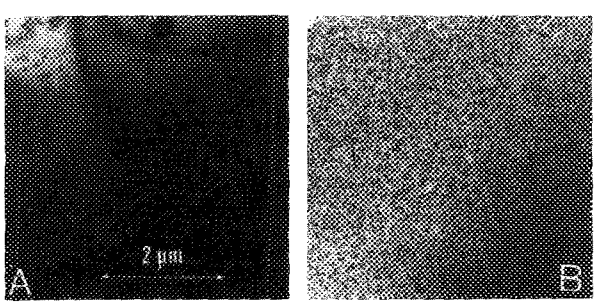

FIG. 17. Plan-view TEM micrographs from Te-implanted (10^{15} cm^{-2}, 100 keV, 25 °C) GaAs annealed (a) in a furnace at 850 °C for 20 min or (b) in an RTA system at 950 °C for 5 s.

ing of the latter complex would also yield an arsenic vacancy. It remains to be established if vacancy complexing with donors and to a lesser extent amphoteric species is the mechanism limiting the electrical activity. Certainly in some Si-doped GaAs samples, infrared absorption has established the presence of a Si-X (X unidentified) complex which was controlling the degree of electrical activity in the material, to a greater extent than simple Si self-compensation.[28] All of this points to the need for spatial control of the GaAs stoichiometry on an atomic scale around implanted, or grown-in, dopants.

ACKNOWLEDGMENTS

The authors acknowledge the contributions to this work by F. Sette and J. E. Rowe with their discussions on EXAFS measurements.

[1]J. P. Donnelly, Nucl. Instrum. Methods **182/183**, 553 (1981).
[2]J. S. Williams, in *Laser Annealing of Semiconductors*, edited by J. M. Poate and J. W. Mayer (Academic, New York, 1982), p. 383.
[3]K. G. Stephens, Nucl. Instrum. Methods **209/210**, 589 (1983).
[4]D. K. Sadana, Nucl. Instrum. Methods B **7/8**, 375 (1985).
[5]H. Nishi, Nucl. Instrum. Methods B **7/8**, 395 (1985).
[6]F. H. Eisen, in *Ion Implantation and Beam Processing*, edited by J. S. Williams and J. M. Poate (Academic, Sydney, Australia, 1984), Chap. 10.
[7]D. V. Morgan and F. H. Eisen, in *Gallium Arsenide*, edited by M. J. Howes and D. V. Morgan (Wiley, New York, 1985), Chap. 5.
[8]K. G. Orrman-Rossiter, S. T. Johnson, and J. S. Williams, Nucl. Instrum. Methods B **7/8**, 448 (1985).
[9]F. Sette, S. J. Pearton, J. E. Rowe, J. M. Poate, and J. Stohr, Phys. Rev. Lett. **56**, 2637 (1986).
[10]F. Sette, S. J. Pearton, J. E. Rowe, and J. M. Poate, Nucl. Instrum. Methods B **19/20**, 408 (1987).
[11]S. J. Pearton, J. S. Williams, K. T. Short, S. T. Johnson, J. M. Gibson, D. C. Jacobson, J. M. Poate, and D. O. Boerma, Mater. Res. Soc. Symp. Proc. **93**, 59 (1987).
[12]A. G. Associates, Sunnyvale, CA 94089.
[13]See, for example, the discussion in C. H. Kang, K. Kondo, J. Lagowski, and H. C. Gatos, J. Electrochem. Soc. **134**, 1261 (1987).
[14]D. E. Davies, Nucl. Instrum. Methods B **7/8**, 387 (1985).
[15]J. P. Biersack and L. G. Haggmark, Nucl. Instrum. Methods **74**, 257 (1980).
[16]K. D. Cummings, S. J. Pearton, and G. P. Vella-Coleiro, J. Appl. Phys. **60**, 166 (1986).
[17]T. Hiramoto, T. Saito, and T. Ikoma, Jpn. J. Appl. Phys. **24**, 2193 (1985).
[18]N. J. Barrett, J. D. Grange, B. J. Sealy, and K. G. Stephens, J. Appl. Phys. **56**, 3503 (1984).
[19]S. S. Kular B. J. Sealy, Y. Ono, and K. G. Stephens, Solid-State Electron. **27**, 83 (1984).
[20]C. M. Wolfe and G. E. Stillman, Appl. Phys. Lett. **27**, 564 (1975).
[21]R. Bensalem and B. J. Sealy, Vacuum **36**, 921 (1986).
[22]B. J. Sealy, N. J. Barret, and R. Bensalem, J. Phys. D **19**, 2147 (1986).
[23]N. Morris and B. J. Sealy, Mater. Res. Soc. Symp. Proc. **126**, 189 (1988).
[24]S. J. Pearton, R. Hull, D. C. Jacobson, J. M. Poate, and J. S. Williams, Appl. Phys. Lett. **48**, 38 (1986).
[25]J. Lindhard, M. Scharff, and H. E. Schiott, K. Dan. Vidensk. Selsk. Mat. Fys. Medd. **33**, 14 (1963).
[26]S. J. Pearton, J. M. Poate, F. Sette, J. M. Gibson, D. C. Jacobson, and J. S. Williams, Nucl. Instrum. Methods B **19/20**, 369 (1987).
[27]D. Pons and J. C. Bourgoin, J. Phys. C. **18**, 3839 (1985).
[28]J. Maguire, R. Murray, R. C. Newman, R. B. Beall, and J. J. Harris, Appl. Phys. Lett. **50**, 516 (1987).